Parameter adaptation in admittance control for stable physical human-robot interaction

Federica Ferraguti, Chiara Talignani Landi, Lorenzo Sabattini, Marcello Bonfè,
Cesare Fantuzzi and Cristian Secchi

***Abstract*— The possibility of adapting online the way a robot interacts with the environment is becoming more and more important. Nevertheless, stability problems arise when the environment (e.g. the human) the robot is interacting with gets too stiff. In this work, we present a strategy for handling the stability issues related to a change of stiffness of the human arm during the interaction with an admittance-controlled robot. Moreover, we introduce a method for detecting the rise of instability and a passivity preserving strategy for restoring a stable behavior.**

I. Introduction

One of the most revolutionary and challenging features of the new generation of robots is physical human-robot interaction (pHRI). In pHRI tasks, robots are designed to coexist and cooperate with humans in applications such as assisted industrial manipulation, collaborative assembly, domestic work, entertainment, rehabilitation or medical applications. In these contexts, due to the desired coexistence of robotic systems and humans in the same workspace, main concerns are related to safety and dependability. A widely used approach consists in implementing interaction control strategies that guarantee a compliant behavior of the robot. In particular, admittance control is typically utilized for controlling industrial robots, that are generally characterized by a stiff and non-backdrivable mechanical structure [1].

For example, admittance control has been used to implement robot manual guidance in [2] and [3], by means of the "walk-through programming" where the human operator becomes the teacher that physically guides the robot throughout the desired trajectory.

When using admittance-controlled robots, instability can arise when interacting with stiff environments [4]. Since humans are dynamic systems characterized by a time-varying impedance, they can behave in a stiff way and, consequently, give rise to instability when interacting with admittance-controlled robot. Instability induces, among other undesired effects, a deviation of the robot from the desired admittance behavior. Furthermore, it produces high amplitude oscillations of the end-effector, undermining the user safety during the interaction. The deviations have to be first promptly detected and then canceled (or reduced) to restore the stability of the system. The adaptation of the parameters of the admittance control is a common strategy for recovering the stability of the interaction as shown, e.g., in [5], [6] and [7].

F. Ferraguti, C. Talignani Landi, L. Sabattini, C. Fantuzzi and C. Secchi are with the Department of Sciences and Methods for Engineering (DISMI), University of Modena and Reggio Emilia, Italy {federica.ferraguti, chiara.talignanilandi, lorenzo.sabattini, cesare.fantuzzi, cristian.secchi}@unimore.it
M. Bonfè is with the Engineering Department, University of Ferrara, Italy marcello.bonfe@unife.it

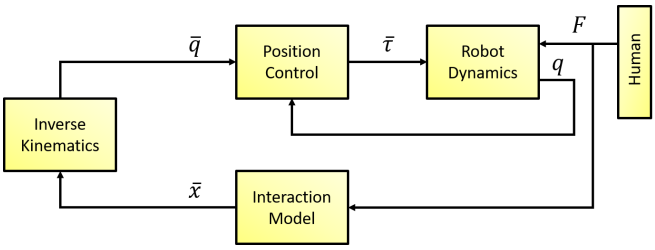

Fig. 1. Control scheme of the admittance control with underlying motion controller. The solution of the interaction model with the input $F(t)$ provides the value $\bar{x}$ which the position-controlled robot must follow, by computing the desired joint positions $\bar{q}$ from inverse kinematics and regulating the joint torque τ to let the actual joint positions q track $\bar{q}$.

In this work we show a novel strategy for detecting the rise of oscillations during the interaction between a human and an admittance-controlled robot and a passivity based parametric adaptation of the admittance for restoring a stable behavior. The proposed adaptation allows to keep the adaptive dynamics similar to the nominal one in order to avoid unbalancing effects and to increase the usability of the system. Preliminary results have been presented in [8] and [9], while in [10] a method for automatically setting the detection threshold using a thorough statistical analysis has been introduced. Moreover, a weighted energy allocation strategy has been proposed in order to consider separately translations and rotations. In this work we present the overall framework and we show the experimental validation of the control architecture.

II. Admittance control and issues in human-robot interaction

Consider a n-degree of freedom (n-DOF) manipulator controlled by using the admittance control scheme shown in Fig. 1. Given a desired interaction model, namely a dynamic relation between the motion of the robot and the force applied by the environment, and given the external force, the admittance equation, via a suitable integration (see, e.g., [11], [12] for explicit passive integration strategies), generates the position and orientation to be used as a reference for a low-level position controller. The goal of the admittance control is to force the robot to behave compliantly with

the environment, according to a given mass-spring-damper system. The elastic part of this system is used to attract the robot end-effector towards a desired pose. However, since we want to address the case of a robotic manipulator manually driven by the human operator, in this paper we do not consider the elastic part of the general admittance control model. Indeed, the user guides the robot by means of the force applied to its end-effector, without directly specifying a desired pose. Let $\bar{x}(t) \in \mathbb{R}^6$ be the set-point computed by the admittance controller and $x(t) \in \mathbb{R}^6$ be the pose of the end-effector, obtained from the joint positions $q(t) \in \mathbb{R}^m$, $m \geq 6$, through the forward kinematics. For ease of notation we will hereafter omit the dependency of $q(t)$ from t. We expect that the low-level position controller is designed and tuned to minimize the tracking error and optimize the dynamic response so that the robot can track a feasible set-point. Thus, we will make the following assumption:

Assumption 1: The low-level position controller is designed and tuned in such a way that $x(t) \simeq \bar{x}(t)$ as long as

$$\begin{aligned} -\dot{\mathcal{X}}(q) \leq \dot{\bar{x}}(t) \leq \dot{\mathcal{X}}(q) \\ -\ddot{\mathcal{X}}(q) \leq \ddot{\bar{x}}(t) \leq \ddot{\mathcal{X}}(q) \end{aligned} \tag{1}$$

where

$$\begin{aligned} \dot{\mathcal{X}}(q) &= \left[\dot{\mathcal{X}}_1, \ldots, \dot{\mathcal{X}}_6\right]^T \in \mathbb{R}^6 \\ \ddot{\mathcal{X}}(q) &= \left[\ddot{\mathcal{X}}_1, \ldots, \ddot{\mathcal{X}}_6\right]^T \in \mathbb{R}^6 \end{aligned} \tag{2}$$

are configuration-dependent velocity and acceleration bounds due to the robot dynamics and the inequalities are component-wise.

We want to force the robot to interact with the environment according to the following desired behavior:

$$M_d \ddot{x}(t) + D_d \dot{x}(t) = F(t) \tag{3}$$

where $M_d \in \mathbb{R}^{6\times6}$ and $D_d \in \mathbb{R}^{6\times6}$ are the desired inertia and damping symmetric and positive definite matrices. The external force $F(t) \in \mathbb{R}^6$ in (3) is assumed to be measured by a 6-DOF force/torque (F/T) sensor attached at the robot wrist flange. The controlled robot behaves as (3) and it is passive with respect to the pair $(F(t), \dot{x}(t))$, as proved in [13].

During the execution of the cooperative task, the robot is coupled with a human operator, whose dynamics (e.g. change of compliance of the arm) can cause deviations from the desired behavior that may produce robot oscillating motions of high amplitude and frequency, making the interaction unsafe for the user ([5]). Thus, the oscillations have to be detected and then the desired behavior has to be recovered.

In order to be able to compensate the destabilizing effects by adapting the parameters, the following, time-varying, interaction model can be implemented:

$$M(t)\ddot{x}(t) + D(t)\dot{x}(t) = F(t) \tag{4}$$

where $M(t) \in \mathbb{R}^{6\times6}$ and $D(t) \in \mathbb{R}^{6\times6}$ are inertia and damping symmetric and positive definite matrices such that $M(0) = M_d$ and $D(0) = D_d$. While increasing the damping is an intuitive and passivity preserving approach since it increases the energy dissipated, changing the inertia is, in general, a non passive operation ([13]). Thus, it may happen that the procedure for stabilizing the interaction makes the admittance dynamics non passive and possibly unstable. Nevertheless, using the following method it is possible to adapt both the damping and inertia parameters in (4) while preserving the passivity of the initial dynamics.

In [8] the following simple heuristic for detecting the rise of an oscillatory behavior during the cooperation has been proposed:

$$\|F(t) - M(t)\ddot{x}(t) - D(t)\dot{x}(t)\| \leq \varepsilon \tag{5}$$

where $\varepsilon \in \mathbb{R}^+$ is an appropriately defined small threshold. When (5) is not satisfied, the robot is considered to be deviating from the interaction model imposed by the admittance control. Unfortunately, since oscillating motions have a high frequency, that corresponds to high values of velocities and accelerations, the threshold indicating such a deviation strongly depends on the maximum velocity and acceleration achievable by the robot and on the time-varying admittance parameters. This makes ε also time-varying and hard to tune. In [9] a novel condition for detecting the rise of high-frequency oscillations that is more robust than (5) has been proposed. However, the value of the detection threshold ε still has to be manually found through post-processing operations.

III. Online detection of rising oscillations in physical human-robot interaction

In order to overcome the drawbacks introduced by the use of real-time computations of (5) to detect the rising oscillations, an improved heuristic and a practical procedure for tuning the detection threshold ε can be used. Let us define the vectors $\dot{\hat{x}}(t) \in \mathbb{R}^6$ and $\ddot{\hat{x}}(t) \in \mathbb{R}^6$ as the tracking error derivatives scaled with respect to the bounds $\dot{\mathcal{X}}$ and $\ddot{\mathcal{X}}$. In particular, the j-th components of the scaled vectors are defined as follows:

$$\dot{\hat{x}}_j(t) = \frac{\dot{\tilde{x}}_j(t)}{\dot{\mathcal{X}}_j(q)} \qquad \ddot{\hat{x}}_j(t) = \frac{\ddot{\tilde{x}}_j(t)}{\ddot{\mathcal{X}}_j(q)} \qquad j = 1, \ldots, 6 \tag{6}$$

where

$$\begin{aligned} \dot{\tilde{x}}(t) &= \dot{\bar{x}}(t) - \dot{x}(t) = \left[\dot{\tilde{x}}_1(t) \ldots \dot{\tilde{x}}_6(t)\right]^T \in \mathbb{R}^6 \\ \ddot{\tilde{x}}(t) &= \ddot{\bar{x}}(t) - \ddot{x}(t) = \left[\ddot{\tilde{x}}_1(t) \ldots \ddot{\tilde{x}}_6(t)\right]^T \in \mathbb{R}^6 \end{aligned} \tag{7}$$

are the first and second order derivatives of the tracking error. Robot velocities and accelerations can be measured using specific hardware (e.g. gyroscopes and accelerometers) or estimated using, for example, the quaternion-based Kalman filter introduced in [14].

Moreover, we introduce the following damping to inertia ratio matrix:

$$R_d(t) = M^{-1}(t)D(t) \tag{8}$$

The improved heuristic can be defined in terms of (6) and (8), as follows:

$$\psi\left(\dot{\hat{x}}(t), \ddot{\hat{x}}(t)\right) = \|\ddot{\hat{x}}(t) + R_d(t)\dot{\hat{x}}(t)\| \leq \varepsilon \tag{9}$$

(9) can be used as the heuristic for detecting online when oscillations occur. Namely, when (9) is not satisfied, we claim that oscillations are rising.

According to the experimental results obtained in [10], the distribution of the detection index $\psi(t)$ can be characterized as a log-normal. Thus, the following procedure can be used for tuning the detection threshold ε:

1) Given initial values of inertia and damping matrices and, therefore, of the desired damping to inertia ratio matrix, the experienced operator applies persistent force stimuli to the admittance-controlled robot to move it in a wide portion of its workspace, while the control system logs the values of $\psi(t)$ for at least 60 seconds.
2) The potential presence of a significant number of outliers in the recorded series of $\psi(t)$ is detected. Indeed, outlying samples are potentially related to undesired oscillations that even the experienced user may have not perceived. Being the log-normal a *skewed* distribution, the outliers detection is based on the adjusted boxplot described in [15]. Following this approach, a sample is considered to be an outlier if it falls outside of the interval:
$$\left[Q_1 - 1.5e^{-4MC}\mathrm{IQR},\ Q_3 + 1.5e^{3MC}\mathrm{IQR}\right] \quad (10)$$
where Q_1 and Q_3 are respectively the first and third quartile of the sampled data, $\mathrm{IQR} = Q_3 - Q_1$ is the interquartile range and MC is the *medcouple*, a robust measure of skewness ([16]). Note that the proposed boxplot formula assumes $MC > 0$, since a log-normal distribution is *right* skewed. If the total number of outliers does not exceed 5% of the sampled data and consecutive outlying samples represent short time intervals (e.g. smaller than 200 ms), it can be concluded that experimental data do not include oscillating behaviors and can be used for the subsequent steps of the tuning procedure.
3) If outliers are negligible and the user acknowledges that the experimental run is valid for the tuning of the threshold, the PDF of $\psi(t)$ is estimated from sampled data. In particular, the parameters of a log-normal distribution are estimated using the following MLE formulas (see [17]):
$$\hat{\mu} = \frac{\sum_{i=0}^{N-1} \ln \psi(i \cdot T)}{N}; \quad \hat{\sigma} = \sqrt{\frac{\sum_{i=0}^{N-1} \left(\ln \psi(i \cdot T) - \hat{\mu}\right)^2}{N}} \quad (11)$$
where T is the sampling period, N is the number of discrete-time samples of $\psi(t)$ collected during the test, $\hat{\mu}$ and $\hat{\sigma}$ are the estimated *location* and the estimated *scale* of the log-normal distribution ([18]), respectively.
4) The threshold ε is fixed as the upper bound of the prediction interval calculated as the value at which the log-normal CDF reaches the confidence level $\alpha = 0.9999$ (chosen with the aim to mostly avoid false positive detections).

IV. Passivity-based methodology for parameter adaptation

As already introduced, the parameters of the admittance control can be adapted to restore the desired behavior of the controlled robot in the presence of high-frequency oscillations, identified according to the technique described in Section III. If the parameters have to be adapted, then the desired interaction model becomes the variable admittance model (4). The main drawback due to the introduction of variable terms in an admittance control scheme is the loss of passivity of the controlled robot (see, e.g., [13]). In order to guarantee the passivity, we exploit the concept of energy tanks that allows to use the (virtual) energy circulating in the controlled system in a flexible and passivity preserving way (see, e.g., [19], [20], [13]). Indeed, the energy dissipated by the system is stored in a virtual energy reservoir, the *tank*, and can be reused for implementing any desired control action in a passivity preserving way. For this purpose, the dynamics (4) is augmented as follows:

$$\begin{cases} M(t)\ddot{x}(t) + D(t)\dot{x}(t) = F(t) \\ \dot{z}(t) = \dfrac{\varphi(t)}{z(t)} P_D(t) - \dfrac{\gamma(t)}{z(t)} P_M(t) \end{cases} \quad (12)$$

where

$$P_D(t) = \dot{x}(t)^T D(t) \dot{x}(t) \qquad P_M(t) = \tfrac{1}{2} \dot{x}(t)^T \dot{M}(t) \dot{x}(t) \quad (13)$$

are the dissipated power due to the damping, and the dissipated/injected power due to the inertia variation, respectively, and $z(t) \in \mathbb{R}$ is the state of the tank. Furthermore, let

$$T(z(t)) = \frac{1}{2} z(t)^2 \quad (14)$$

be the energy stored in the tank. We will hereafter assume that $\exists \delta, \bar{T}$, with $0 < \delta < \bar{T}$, such that $\delta \leq T(z(t)) \leq \bar{T}$, $\forall t$. The upper bound is guaranteed by the parameters $\varphi(t) \in \{0, 1\}$ and $\gamma(t) \in \{0, 1\}$ that disable the energy storage in case a maximum, application dependent, limit $\bar{T} \in \mathbb{R}^+$ is reached. It is necessary to bound the available energy because, if there were no bounds, the energy could become very big as time increases and, even if the system keeps on being passive, it would be possible to implement practically unstable behaviors ([21]). In particular,

$$\varphi(t) = \begin{cases} 1 & \text{if } T(z(t)) \leq \bar{T} \\ 0 & \text{otherwise} \end{cases} \quad (15)$$

enables/disables the storage of dissipated energy, while

$$\gamma(t) = \begin{cases} \varphi & \text{if } \dot{M}(t) \leq 0 \\ 1 & \text{otherwise} \end{cases} \quad (16)$$

enables/disables the injection $\left(\dot{M}(t) \leq 0\right)$ of energy in the tank due to the inertia variation but it always allows to extract $\left(\dot{M}(t) > 0\right)$ energy from the tank. The lower bound, required for avoiding singularities in (12), is guaranteed by carefully planning/forbidding the extraction of energy when $T(z(t)) = \delta$ is reached. Notice that the extraction of energy

is due only to $P_M(t)$. The tank initial state is set to $z(0)$ such that $T(z(0)) > \delta$.

It can be formally proven that if $T(z(t)) \geq \delta$ for all $t \geq 0$, the system (12) is passive with respect to the pair $\left(F(t), \dot{\tilde{x}}(t)\right)$ [10]. Thus, as long as there is energy available in the tank, it is possible to implement any kind of inertia variation. Nevertheless, it is important to guarantee that the variation of the inertia does not deplete the tank. Indeed, if this happens, all the active behaviors (e.g. increasing of inertia) would be stopped and this would lead to unwanted behaviors (e.g. oscillations) in the cooperative system. In the following we propose a condition on the variation of the inertia that guarantees that the tank never depletes and, as a consequence, that the system remains passive.

We assume that the inertia variations take place in predefined finite intervals (e.g. when the user stiffens his/her arm). As clearly shown in (12) and in (13), energy can be extracted by the tank only if $\dot{M}(t) > 0$. Thus, it is necessary to bound the increase of inertia depending on the energy stored in the tank.

Since the desired inertia and damping are parameters that can be freely chosen, provided that they are symmetric and positive definite matrices, we consider the following assumption.

Assumption 2: The desired inertia and damping in (4) are diagonal matrices and they are defined as

$$\begin{aligned} M(t) &= \operatorname{diag}\{m_1(t), \ldots, m_6(t)\} \\ D(t) &= \operatorname{diag}\{d_1(t), \ldots, d_6(t)\} \end{aligned} \tag{17}$$

Since $M(t)$ is diagonal, $\dot{M}(t)$ is diagonal too and its eigenvalues are the elements on the diagonal.
With this assumption, we can decouple the different components (e.g. the translational components from the rotational ones).

A condition on the inertia variations that allows to preserve passivity, with a weighted distribution of the energy extracted from the tank within the adaptation interval, is derived and stated in [10] as follows:

$$\dot{m}_j(t) \leq \bar{\dot{m}}_j \leq \frac{2\alpha_j(T(a) - \delta)}{\bar{\dot{\mathcal{X}}}_j^2 (b - a)} \quad \forall j = 1, \ldots, 6 \tag{18}$$

where $[a, b]$ is the time interval of the inertia variation, $\bar{\dot{m}}_j$ $(j = 1, \ldots, 6)$ are bounds on $\dot{m}_j(t)$ for all $t \in [a, b]$ and $\bar{\dot{\mathcal{X}}}_j = \max_q \dot{\mathcal{X}}_j(q)$ $(j = 1, \ldots, 6)$ are component-wise upper bounds on the robot velocity limits defined in Assumption 1. The vector $\mathcal{A} = \{\alpha_1, \ldots, \alpha_6\}$, is a vector of weights defined such that:

$$\sum_{j=1}^{6} \alpha_j = 1 \tag{19}$$

This newer formulation of the passivity-preserving adaptation law, with respect to the one used in [9], [8], allows to take into account that the velocity bounds of the robot may be quite different on the different DOFs, especially comparing translational and rotational ones. Thanks to the component-wise definition of the inertia variation bound and to a proper choice of the weights vector $\mathcal{A}$, the adaptation of the admittance parameters related to each DOF can be tuned more precisely, according to the features of the robot and to the desired task. Intuitively, lower weights should be specified for the components related to rotational DOFs, whose corresponding elements on the diagonal of $M(t)$ tends to be smaller than those related to translational DOFs (i.e. the values in the inertia tensor of a rigid body are, in general, quantitatively smaller than its mass). On the other hand, the oscillating behavior of the human-robot interaction can be counteracted with smaller inertia variations on those DOFs for which higher velocities are admissible. More details on the tuning of the weights vector are given in [10].

A. Algorithm for parameter adaptation in admittance control

The previous section provided a possible way for using (18) to adapt the parameters of the admittance control to recover a stable behavior of the human-robot interaction when oscillations are detected. In the following will be described a procedure for parameter adaptation, that allows to increase the parameters only when it is required due to the detection of rising oscillations, but then restores the desired interaction model when such oscillations disappear (e.g. due to a relaxation of the operator's arm). The parameters will be adapted according to the component-wise passivity-preserving bound defined by (18). The algorithm will be provided in the discrete-time domain in order to be implementable on a real robotic system. The conditions on the time derivatives stated so far can be approximated using the corresponding difference quotient for a sufficiently small sampling period. We will then consider a set of time intervals $[t_i, t_{i+1}]$, with $i = 1, 2, \ldots$ and such that $t_{i+1} - t_i = \Delta t$, within which the parameter adaptation takes place.

Once rising oscillations have been detected, the algorithm allows to compute the variation of the inertia that satisfies the passivity constraints and the stability of the system is recovered. The variation of the damping is performed according to a constant damping to inertia ratio ($R_d(t) = R_d(0), \forall t \geq 0$). Thus, the first step of the algorithm is the computation of the damping to inertia ratio according to (8) and based on the desired inertia matrix $M(0)$ and damping matrix $D(0)$.

Then, at each time instant t_i, the detection index defined in (9) is computed. If oscillations are rising, (9) is not satisfied and the oscillatory behavior is detected. A vector ζ is created to store all the instants in which oscillations are detected. Thus, a new element ζ_k is inserted in ζ and it is associated to the current instant of time t_i which corresponds to the instant of detection. In this case, the admittance parameters have to be adapted for restoring the stability of the system. In particular, integrating (18), we obtain that each component of the inertia matrix can be passively increased as follows

$$m_j(t_{i+1}) - m_j(t_i) = \frac{2\alpha_j(T(t_i) - \delta)}{\bar{\dot{\mathcal{X}}}_j^2} \quad \forall j = 1, \ldots, 6 \tag{20}$$

It is worth noting that (20) represents the maximum allowed

inertia variation, based on the energy contained in the tank at time $t = t_i$. In practical cases, this value can be very large: thus, direct application of (20) would lead to an excessively large inertia variation. For this reason, we define an upper-bound $\Delta M = \text{diag}\{\bar{m}_1, \cdots, \bar{m}_6\}$ on the allowed inertia variation as follows:

$$m_j(t_{i+1}) - m_j(t_i) \leq \bar{m}_j \quad \forall j = 1, \ldots, 6 \tag{21}$$

Under such a condition, the amount of variation of the inertia can be computed component-wise as the minimum between the allowed inertia variation (20) and the upper-bound (21):

$$s_j = \min \left\{ \frac{2\alpha_j (T(t_i) - \delta)}{\bar{\dot{\mathcal{X}}}_j^2}, \bar{m}_j \right\} \quad \forall j = 1, \ldots, 6 \tag{22}$$

The empirical definition of the bounds $\bar{m}_j$ is a practical necessity and has been exploited in the experiments described in [9], [8] also to take into account that some DOFs (i.e. generally rotational ones) may require smaller values of inertia variations. However, the newer definition of the inertia adaptation law, based on the weighted distribution of the tank energy, allows to modulate more precisely the inertia variations, thanks to the choice of the weights vector and the component-wise scaling by the velocity bounds $\bar{\dot{\mathcal{X}}}_j$. Indeed, the conservative bounds $\bar{m}_j$ are rarely enforced.

The single components computed in (22) are then used to fill the matrix of inertia variation as follows:

$$S_i = \text{diag}\{s_1, \ldots, s_6\} \quad \forall i = 1, 2, \ldots \tag{23}$$

The final part of the algorithm is the actual variation of the admittance parameters. The inertia variation is computed as follows:

$$M(t_{i+1}) = M(0) + \sum_{p=0}^{k} S_p \beta^{(t_{i+1} - (\tau_p + \Delta t))} \tag{24}$$

where β ($0 < \beta \leq 1$) is a forgetting factor that allows to gradually restore the desired interaction model (3). Indeed, the presence of the forgetting factor β in the second term in the right-hand side of (24) makes the effect of each inertia increase negligible after a certain amount of time. In particular, this time is larger for higher values of β. Note that the inertia increases only at each time instant when a deviation is detected, as a consequence of (24). In all the other instants, the inertia only decreases and this has been shown in [8] to be a passivity-preserving operation.

Finally, the damping is updated preserving the constant damping to inertia ratio as follows:

$$D(t_{i+1}) = R_d(0) M(t_{i+1}) \tag{25}$$

More details on the algorithm can be found in [10].

V. Experiments

In order to demonstrate the effectiveness of the overall detection and adaptation strategy, we present experimental results that show how the heuristic introduced in Section III detects the oscillatory behavior of the robots and the way

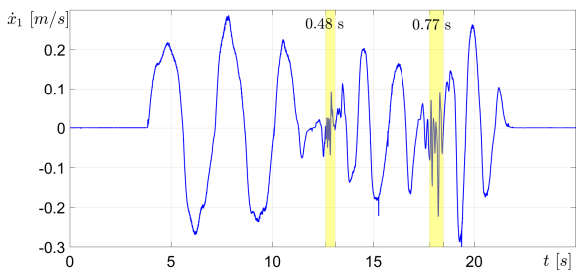

(a) Velocity of the robot along the considered translational DOF

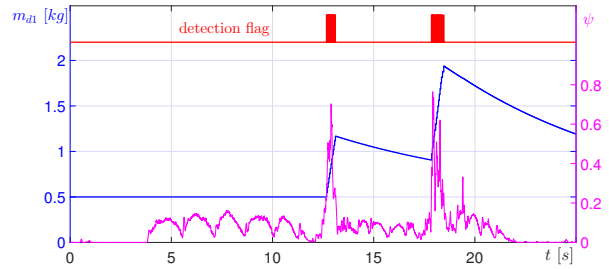

(b) Evolution over time of the detection index $\psi(t)$ (magenta line), and of the subsequent inertia adaptation (blue line). A detection flag (red line) is added to show when the heuristic detects that oscillations are rising.

Fig. 2. Detection and adaptation of the rising oscillations using the proposed method.

stability is restored thanks to the adaptation strategy presented in Section IV. These specific experiments have been performed restricting robot motion to only one translational DOF. The inertia and damping initial parameters have been set equal to $m(0) = 0.5\ kg$ and $d(0) = 5\ {}^{kg}/_{m^2}$, since these values have been found in [5] to be the minimum stable admittance gains for a KUKA LWR 4+, which is also the robot used in our experiments. In these conditions, the detection threshold has been properly tuned with the proposed procedure and it resulted $\varepsilon = 0.22$. Whenever the user excessively stiffens his/her arm, high-frequency oscillations appear in the velocity of the robot (Figure 2(a)). Figure 2(b) shows, in magenta, the evolution over time of the detection index $\psi(t)$ as defined in (9). A boolean detection flag is depicted with a red line in Figure 2(b). As it can be seen, the rising oscillations are rightly detected and the inertia (blue line) is adapted accordingly. As shown in Figure 2(a), when an oscillating behavior arises (yellow regions), the adaptation of the parameters allows to stabilize the system $0.48\ s$ after the occurrence of the first oscillation and $0.68\ s$ after the occurrence of the second oscillation. Obviously, the difference in the adaptation times is due to the different attitude of the operator during the interaction, the different amplitude of the oscillations and, finally, to the starting values of the parameters when the adaptation is performed. However, thanks to a usability study we could verify that, from the user perspective, all the adaptation periods were sufficiently short amounts of time, since the adaptation of the parameters was achieved before the user could actually feel the rising oscillations.

VI. Conclusions

Admittance control is a widely used approach for guaranteeing a compliant behavior of the robot in physical human-robot interaction. When an admittance-controlled robot is coupled with a human operator, the dynamics of the human can cause deviations from the desired behavior, that is the one imposed by the admittance control. The deviations result in high amplitude oscillations of the robot end-effector that may render the interaction with the robot unsafe for the user.

In this work we presented a strategy for detecting the rising oscillations and adapting the parameters of the admittance control for restoring the stability. To detect the rising oscillations, a heuristic has been defined. A procedure for automatically tuning the detection threshold used in the heuristic has been proposed, by exploiting statistical methods. We then provided an algorithm for adapting the parameters of the admittance control when it is necessary, i.e. when a rising oscillation is detected, while preserving the passivity of the system. The parameters are gradually restored when the destabilizing factors are no longer active.

References

[1] L. Villani and J. De Schutter, "Force control," in *Springer Handbook of Robotics*, B. Siciliano and O. Khatib, Eds. Springer Berlin Heidelberg, 2008, ch. 7.

[2] C. Talignani Landi, F. Ferraguti, C. Secchi, and C. Fantuzzi, "Tool compensation in walk-through programming for admittance-controlled robots," in *Proceedings of the Annual Conference of IEEE Industrial Electronics Society*, Firenze, Italy, 2016.

[3] F. Ferraguti, C. Talignani Landi, C. Secchi, C. Fantuzzi, M. Nolli, and M. Pesamosca, "Walk-through programming for industrial applications," *Procedia Manufacturing*, vol. 11, pp. 31–38, 2017.

[4] S. Eppinger and W. Seering, "On dynamic models of robot force control," in *Proceedings of the IEEE International Conference on Robotics and Automation*, 1986.

[5] F. Dimeas and N. Aspragathos, "Online stability in human-robot cooperation with admittance control," *IEEE Transactions on Haptics*, vol. 9, no. 2, pp. 267–278, 2016.

[6] A. Campeau-Lecours, M. Otis, P. Belzile, and C. Gosselin, "A time–domain vibration observer and controller for physical human–robot interaction," *Mechatronics*, vol. 36, pp. 45–53, June 2016.

[7] A. Lecours, B. Mayer-St-Onge, and C. Gosselin, "Variable admittance control of a four-degree-of-freedom intelligent assist device," in *Proceedings of the IEEE International Conference on Robotics and Automation*, Minnesota, USA, 2012.

[8] C. Talignani Landi, F. Ferraguti, L. Sabattini, C. Secchi, and C. Fantuzzi, "Admittance control parameter adaptation for physical human-robot interaction," in *Proceedings of the IEEE International Conference on Robotics and Automation*, Singapore, 2017.

[9] C. Talignani Landi, F. Ferraguti, L. Sabattini, C. Secchi, M. Bonfè, and C. Fantuzzi, "Variable admittance control preventing undesired oscillating behaviors in physical human-robot interaction," in *Proceedings of the IEEE International Conference on Intelligent Robots and Systems*, Vancouver, Canada, 2017.

[10] F. Ferraguti, C. T. Landi, L. Sabattini, M. Bonfè, C. Fantuzzi, and C. Secchi, "A variable admittance control strategy for stable physical human–robot interaction," *The International Journal of Robotics Research*, vol. 38, no. 6, pp. 747–765, 2019.

[11] M. De Stefano, R. Balachandran, J. Artigas, and C. Secchi, "Reproducing physical dynamics with hardware-in-the-loop simulators: A passive and explicit discrete integrator," in *Proceedings of the IEEE International Conference on Robotics and Automation*, May 2017, pp. 5899–5906.

[12] M. De Stefano, J. Artigas, and C. Secchi, "A passive integration strategy for rendering rotational rigid-body dynamics on a robotic simulator," in *Proceedings of the IEEE/RSJ International Conference on Intelligent Robots and Systems*, Sept 2017, pp. 2806–2812.

[13] F. Ferraguti, N. Preda, A. Manurung, M. Bonfè, O. Lambercy, R. Gassert, R. Muradore, P. Fiorini, and C. Secchi, "An energy tank-based interactive control architecture for autonomous and teleoperated robotic surgery," *IEEE Transactions on Robotics*, vol. 31, no. 5, pp. 1073–1088, 2015.

[14] S. Farsoni, C. Talignani Landi, F. Ferraguti, C. Secchi, and M. Bonfè, "Compensation of load dynamics for admittance controlled interactive industrial robots using a quaternion-based kalman filter," *IEEE Robotics and Automation Letters*, vol. 2, no. 2, pp. 672–679, April 2017.

[15] M. Hubert and E. Vandervieren, "An adjusted boxplot for skewed distributions," *Computational Statistics & Data Analysis*, vol. 52, no. 12, pp. 5186 – 5201, 2008.

[16] G. Brys, M. Hubert, and A. Struyf, "A robust measure of skewness," *Journal of Computational and Graphical Statistics*, vol. 13, no. 4, pp. 996–1017, 2004.

[17] B. Ginos, "Parameter estimation for the lognormal distibution," Master's thesis, Brigham Young University, 2009.

[18] N. Johnson, S. Kotz, and N. Balakrishnan, *Continuous Univariate Distributions*, 2nd ed., ser. Probability and Mathematical Statistics. Wiley, 1995, vol. 1 and 2.

[19] C. Secchi, S. Stramigioli, and C. Fantuzzi, "Position drift compensation in port-hamiltonian based telemanipulation." in *Proceedings of the IEEE/RSJ International Conference on Intelligent Robots and Systems*, 2006, pp. 4211–4216.

[20] M. Franken, S. Stramigioli, S. Misra, C. Secchi, and A. Macchelli, "Bilateral telemanipulation with time delays: A two-layer approach combining passivity and transparency." *IEEE Transactions on Robotics*, vol. 27, no. 4, pp. 741–756, 2011.

[21] D. Lee and K. Huang, "Passive-set-position-modulation framework for interactive robotic systems," *IEEE Transactions on Robotics*, vol. 26, no. 2, pp. 354–369, April 2010.